IEEE Access
Multidisciplinary | Rapid Review | Open Access Journal

Received January 21, 2020, accepted February 4, 2020, date of publication February 14, 2020, date of current version February 26, 2020.

Digital Object Identifier 10.1109/ACCESS.2020.2974048

Interference Solutions for the Deployed 2D Optical Coding PON Link Health Detection System With Massive Densely Distributed Customers

ZHIQUN GE AND XIAOHAN SUN

National Research Center for Optical Sensing/Communication Integrated Networking, School of Electronic Science and Engineering, Southeast University, Nanjing 210096, China

Corresponding author: Xiaohan Sun (xhsun@seu.edu.cn)

This work was supported by the National Natural Science Foundation of China under Grant 61271206.

ABSTRACT To process the complex link state signals and obtain the accurate failure decision criterion in the deployment of two-dimensional optical coding link health detection system to an actual PON system with massive densely distributed customers, we develop a customer distribution model which divide interference customers into two categories: sparse and dense distribution, and propose a code allocation rule by changing the connection between the output ports of encoder and access customers. Simulation results show that in 128-customer system with 2km^2 coverage, customer interference probability is reduced by 0.129. The customer distribution model and the code allocation rule are demonstrated by experiment, and the results show that customer interference is significantly mitigated by using code allocation.

INDEX TERMS Passive optical network (PON), link health detection system (LHDS), two-dimensional (2D) optical coding, customer interference.

I. INTRODUCTION

Next generation passive optical network stage 2 (NG-PON2) are considered to be the best solution to meet the increasing demand in data consumption by fixed broadband customers and fifth-generation mobile communication based on the advantage of higher capacity, longer reach, larger splitting ratio, and services convergence of multiple scenarios, such as traditional broadband access, mobile backhaul/fronthaul and PtP-WDM services [1], [2]. In view of the high-level requirements of network protection for NG-PON2 systems, monitoring of physical layer is an important guarantee to the reliability of NG-PON2 systems [2]. Although optical time domain reflectometry (OTDR) has been widely used in troubleshooting of fiber damage and fracture, it is not effective to detect the fault in the distribution fiber [3], [4].

To address the monitoring issue of the distribution fiber behind the optical splitter in PONs, many OTDR-based monitoring schemes have been proposed such as those based on conventional OTDR and digital signal processing techniques [5], tunable photon counting OTDR [6], optical transceiver monitoring [7], and embedded OTDR [8]. In [5], [6], signal processing techniques are introduced to improve the accuracy and dynamic range of OTDR, and achieve the fast and accurate determination of faults in the distribution fiber. However, the superposition of backscattered signals from all fiber branches in OTDR-based monitoring schemes restricts the customer capacity [9]. To improve the customer capacity, a few monitoring schemes based on tunable or multi-wavelength OTDR with FBGs are proposed [10]–[12]. In [10], [11], tunable OTDR is assisted with FBGs deployed in front of the monitored customers, which reflect the OTDR probe signal. The decrease of the reflection peak in the OTDR trace indicates the faulty fiber branch. A code division multiplex-based dual-OTDR traces comparison scheme is proposed in [12]. However, the spectral efficiency in these schemes is relatively low, thus it will occupy abundance monitoring channels in high splitting ratio NG-PON2 systems.

Meanwhile, optical coding-based monitoring schemes, which mainly use mature passive optical components to generate pulse codes for the monitored customers, draw more

The associate editor coordinating the review of this manuscript and approving it for publication was Francesco Musumeci.

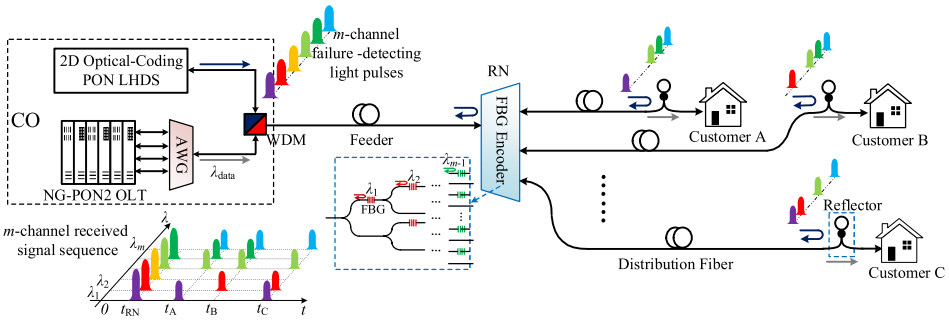

FIGURE 1. The schematic diagram of PON-LHDS utilizing an FBG-based 2D optical-coding scheme. The failure-detecting light pulses are encoded by the FBG encoder and a unique code is allocated to each customer. The FBG encoder reflection signal and customers' codes are sequentially transmitted back.

attentions based on the advantages in monitoring capacity, system cost and potential scalability [3], [9]. However, some difficulties still exist in the actual deployment of such systems. A periodic coding scheme is proposed in [13], [14], and an analytical expression for the average number of false detections is derived in [15]. With the increase of network size, the periodic codes are difficult to be distinguished because of their superposition, thus this scheme suffers from high false detections in high-density PONs. An optical frequency hopping/periodic coding-based centralized PON monitoring scheme is proposed in [16], in which the superposition of periodic codes is reduced in some extent. A simplified method for PON monitoring based on FBGs is proposed, in which FBGs are deployed near vulnerable network locations along the network pathway [17]. However, the vulnerable network locations are not explicitly defined, and the distributed FBGs increase the difficulties of system deployment and retro-fitting to the legacy network. In [18], a novel optical coding scheme based on a single wavelength FBG with different spectral bandwidth is proposed. However, the superposition of the reflection signals will be serious in high-density PONs since only one wavelength is used for monitoring. In [19], an optical pulse width modulation based TDM-PON monitoring scheme utilize an asymmetric loop located in front of the optical network unit (ONU) to generate pulse codes. However, the encoder is located at the customer side in this scheme and a variety of encoders need to be prepared separately, which increase the deployment difficulty and system cost.

In [20], we proposed a remote 2D optical coding PON link health detection system (LHDS) as shown in Fig. 1. Unlike previous optical coding schemes, the design that FBG encoder located in the remote node (RN) reduces system complexity and deployment cost, and makes it easier to synchronize and process the link state signals. Furthermore, in [21], we investigated the dynamic interaction process between the failure-detecting light pulse and 2D optical encoder due to the central wavelength shift, deduced the performance variation of the failure-detecting light pulse passing through FBGs, and analyzed the potential effect of the central wavelength shift on the link state recognition.

In view of the large-scale optical access network systems with massive densely distributed customers in China, the accuracy of real-time PON link monitoring must be guaranteed. Customers of optical access network in China, both business users and residential users, are often densely distributed in the commercial street or the residential quarter, thus the interference issue is serious. After interaction with massive customers, the failure-detecting light pulses containing a large amount of customers' state information are complex and worth to be analyzed and processed in depth. Otherwise, it is difficult to find the accurate decision criterion for massive customers' link states in the system. From the perspective of obtaining the accurate failure decision criterion of PON link monitoring system, it is of great significance to carry out the research of interference issues in depth, and provide effective improvement or compensation solutions. In the field trial of the proposed 2D optical coding LHDS deployed in the actual PON system with massive densely distributed customers, the customer interference issue, which is manifested in the superposition of the link state signals from several customers with similar link length, remains to be solved. On the one hand, the link state signals of interference customers may overlap partially or completely depending on their link length difference and the width of the failure-detecting light pulse. On the other hand, the signal amplitudes from different customers are various due to the different insertion loss, even the signal from one customer may change with the central wavelength shift. Different signal overlapping shapes and various signal amplitudes of the interference customers bring difficulties in the partition of link states. Therefore, we try to establish the customer probability distribution model and find out the impact of customer interference by exploring the relationship between the signal overlapping and the system parameters such as the width of the failure-detecting light pulse, customer link length and customer access port, so as to provide the operators with a secure and reliable optical link monitoring approach.

The rest of this paper is organized as follows: In Section II, we propose a customer distribution model and theoretically derive the customer interference probability. Interference customers are divided into two categories: dense and sparse

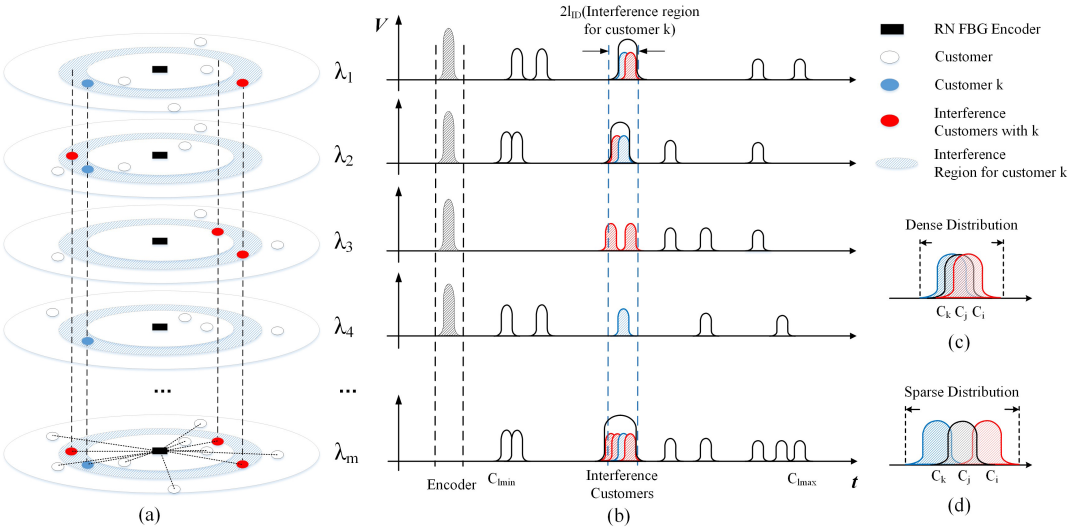

FIGURE 2. Customer distribution model: (a) customer distribution in different wavelength channel; (b) the received light pulses sequence; (c) dense distribution state; (d) sparse distribution state.

distribution states, according to the relationship between signal overlapping and customer link length. The code allocation rule for these two categories of interference customers is proposed for reducing customer interference and false alarm rate. In Section III, the impact of the system parameters: the width of the failure-detecting light pulse, customer capacity and the area of network coverage on the customer interference probability is investigated by simulation. In Section IV, the feasibility of the code allocation rule is demonstrated and an optimal threshold for interference customers is derived.

II. ANALYSIS FOR CUSTOMER INTERFERENCE

A. CUSTOMER DISTRIBUTION MODEL

The deployment of NG-PON2 systems is highly dependent on the customer distribution in the network. In general, the customer distribution depends on the deployment scenario and varies with the customer's type and quantity. The distances from RN to customers in NG-PON2 systems have significant regional characteristics, such as those for FTTH, FTTB, mobile fronthaul. The uniform distribution is an analytically tractable distribution, and provides a reasonable match with the practical PON systems [22], [23]. For multi-dwelling units PON topology which is common in Europe and Asia, the customer distribution is in good agreement with the uniform distribution; nevertheless, in North America where the domination structure is single-family-dwelling units PON topology, the customer density first increases and then decreases along with the increase of distance from RN to customers, not quite consistent with the uniform distribution [22]. However, the ascending portion of the customer density which is much more worthy to study for the customer interference, can be described by the uniform distribution.

Therefore, we assume a uniform distribution of customers over a circular region from RN to all customers as Fig. 2(a) and RN is located in the center. The number of monitoring wavelength channels in PON-LHDS is m and thus the customer capacity is up to 2^{m-1}. For any customer k, a circle is used to represent it and the distance from its center to RN is the link length l_k. Fig. 2(a) illustrates the customer distribution in different wavelength channels. The radius of customer is determined by the width σ_t of the failure-detecting light pulse. The longest link length is l_{max}, and the shortest one is l_{min}. Fig. 2(b) shows the 2D coded signal sequence in one detection period received by the m-channel receiver. Considering that the distance from optical line terminal to customers is usually less than 20 km, the pulse broadening caused by the fiber dispersion can be neglected. Therefore, the width of each pulse in the signal sequence is still σ_t. The FBG encoder reflection signal is first received, and then the customers' reflection signals arrive at the receiver module one after another according to the length of their branch links.

B. PROBABILITY OF CUSTOMER INTERFERENCE

Two interference conditions should be met if customers interfere with others. First, the link state of such customers should be intact, i.e., without fiber fault. In our analysis, we assume that the fiber fault probability ζ of each customer is independent and equal. The second condition is that the length difference ΔL of such customers should be smaller than interference distance l_{ID} which is directly determined by σ_t. Interference distance can be written as $l_{ID} = c\sigma_t/2n_{eff}$, where n_{eff}, c are the effective refractive index and light speed in the fiber core, respectively. Accordingly, for any customer k, customers with link length in interference region ($l_k - l_{ID}$, $l_k + l_{ID}$) can interfere with customer k.

Considering the uniform distribution shown in Fig. 2(a), customers are evenly distributed in a region ranging from l_{min} to l_{max}, and the distribution of customers is independent and

identically distributed, thus the probability density function of customer distribution as a function of the link length l can be expressed by

$$\rho(l) = \frac{2l}{l_{\max}^2 - l_{\min}^2} \tag{1}$$

Therefore, in the interval of $(l - l_{ID}/2, l + l_{ID}/2)$, the probability of existence of one customer can be written as

$$F(l) = \frac{lc\sigma_t}{n_{eff}\left(l_{\max}^2 - l_{\min}^2\right)} \tag{2}$$

For any number of customers, if their link length fall within the interval of $(l - l_{ID}/2,\ l + l_{ID}/2)$, it means that their length difference is less than l_{ID} and they satisfy the interference conditions. Assuming the number of the interference customers is η $(2 \le \eta \le 2^{m-1})$, the event of η customers interfering is independent, thus the probability of customer interference is the sum of the interference probability from 2 to 2^{m-1} customers [24]. For the event of η customers interfering, two requirements need to be satisfied that η customers should locate in the interval of $(l - l_{ID}/2, l + l_{ID}/2)$ and the rest $2^{m-1} - \eta$ customers should be out of the interval. Therefore, the probability of customer interference can be written as

$$P = \sum_{\eta=2}^{2^{m-1}} [F(l)\,(1-\zeta)]^{\eta}\,[1 - F(l)]^{2^{m-1}-\eta} \tag{3}$$

III. CODE ALLOCATION RULE

From the received light pulses sequence shown in Fig. 2(a) and (b), we find that several customers lie in the interference region of customer k, but the overlapping situation of their signals in different wavelength channels is different. Different signal overlapping shapes of the interference customers lead to complicated partition of link states. Various signal amplitudes of different customers also bring difficulties in the determination of accurate decision criterion for link state recognition. High degree of signal overlapping from the similar link length customers will increase the difficulty of link state partition. Besides, some groups of output ports may share the same code leading to false alarm. The same code type is defined in the analysis of false alarm rate in [25]. Therefore, a proper code allocation scheme is urgently needed to reduce the signal overlapping as much as possible and to prevent potential false alarm due to the same code type.

We try to mitigate customer interference by switching or changing the connection between the output ports of encoder and access customers. For example, if (λ_1, λ_m), (λ_2, λ_m) and (λ_3, λ_m) are allocated to three customers with similar link length, λ_1, λ_2 and λ_3 can be used to determine these three customers' link state, respectively. In other words, these three wavelengths are considered to be the characteristic wavelength, which can be directly used to the link state recognition without considering the interference issues. Therefore the probability of customer interference after code allocation

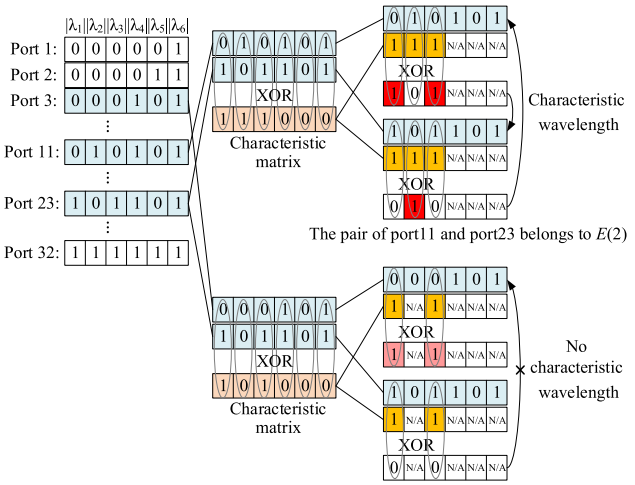

FIGURE 3. The solving process of $E(2)$ in a 6-wavelength PON-LHDS.

can be written as

$$P_{CA} = \sum_{\eta=2}^{2^{m-1}} [F(l)(1-\zeta)]^{\eta}[1-F(l)]^{2^{m-1}-\eta}\left[1 - \frac{E(\eta)}{C_{2^{m-1}}^{\eta}}\right] \tag{4}$$

where the term $C_{2^{m-1}}^{\eta} = (2^{m-1})!/[\eta!(2^{m-1} - \eta)!]$ represents all the possible combinations of codes among a set of 2^{m-1} codes, and the term $E(\eta)$ is the number of combinations of η codes for which all of their elements can have their unique distinctive wavelength (i.e. characteristic wavelength). According to the structure of FBG encoder, in m-wavelength PON-LHDS that supports 2^{m-1} customers, the wavelengths set for port N can be described as

$$N = 2^{m-2} \cdot |\lambda_1| + \cdots + 2^0 \cdot |\lambda_{m-1}| + |\lambda_m| \tag{5}$$

where $|\lambda|$ equals to 1 or 0, depending on whether the port contains λ wavelength signal or not. $|\lambda_m|$ is always 1 because every port contains λ_m wavelength signal. Therefore, the code for port N can be described by a $1 \times m$ matrix $[|\lambda_1|, |\lambda_2|, \ldots, |\lambda_m|]$. Fig. 3 illustrates the solving process of $E(2)$ in a 6-wavelength PON-LHDS. As shown in Fig. 3, in the first step, the characteristic matrix is derived by the XOR of the matrixes of two ports. Then in the second step, the characteristic wavelength of port 11 which is highlighted in red is derived by the XOR of the characteristic matrix and the matrix of port 23, while the zeros in the characteristic matrix are not involved in the second step of calculation. As long as each port has its own characteristic wavelength, the code pair of these two ports belongs to $E(2)$. The code pair of port 3 and port 23 doesn't belong to $E(2)$ because port 3 doesn't have the characteristic wavelength. The value of $E(\eta)$ was obtained by traversing through all the possible code pairs. From Eq. (4), $E(\eta)$ plays an important role in customer interference. Note that $E(\eta)$ decreases with the increase of η, and when η is above $m-1$, $E(\eta)$ equals to zero. In other word, when the number of interference customers is more than $m-1$,

the overlapping degree of signals from these interference customers is relatively high in all wavelength channels. Although for more than $m-1$ interference customers, code allocation cannot contribute to the reduction of customer interference probability, its main purpose is to make sure that any link fault caused by one or more customers has its unique signal characteristic in the received signals, so as to avoid the same code type.

According to the link length difference of the interference customers, we divide all kinds of interference customers into two categories: dense and sparse distribution states. As shown in Fig. 2(c), if customer k and customer i interfere with each other and customer j lies between customer k and customer i, i.e. $l_k \leq l_j \leq l_i$ and $\Delta L_{ki} < l_{ID}$. In this case, customer i, j, k belong to dense distribution state and they interfere with each other. Furthermore, if $l_k \leq l_{k+1} \leq \cdots \leq l_{k+m}$ and $\Delta L_{(m)} = l_{k+m} - l_k < l_{ID}$, customer k to $k+m$ belong to dense distribution state. Fig. 2(d) illustrates another situation that customer j also lies between customer k and customer i, but $\Delta L_{ki} > l_{ID}$, which means that in a sense customer k do not interfere with customer i. In other words, if $\Delta L_{(1)} = l_{k+1} - l_k < l_{ID}$ and $\Delta L_{(2)} = l_{k+2} - l_k > l_{ID}$, customer k to $k+2$ belong to sparse distribution state.

In sparse distribution state, non-adjacent customers actually do not interfere, thus what we have to do is to prevent the interference of adjacent customers by allocating each customer one characteristic wavelength to be its identity. For example in 6-wavelength PON-LHDS, if customer 1 to 5 belong to the sparse distribution and $l_1 < l_2 < l_3 < l_4 < l_5$, port 6($\lambda_3$, λ_5, λ_6), 10(λ_2, λ_5, λ_6), 19(λ_1, λ_4, λ_6), 21(λ_1, λ_3, λ_6) and 18(λ_1, λ_5, λ_6) can be assigned to them by ordinal. In this case, λ_3, λ_2, λ_4, λ_3, λ_5 will be the characteristic wavelengths to recognize these five customers' link state, respectively.

The code allocation rule for interference customers of dense distribution state is as follows. Assuming that customer x, y, p and q belong to dense distribution state. If the ports they are connected to satisfy the following conditions in the Eq. (6), customer x and y will share the same code with p and q, which means we may not differentiate the link failure caused by x and y from that caused by p and q.

$$\begin{cases} N_x + N_y = N_p + N_q \\ \psi_{Nx} + \psi_{Ny} = \psi_{Np} + \psi_{Nq} \end{cases} \tag{6}$$

where Ψ_N denotes the number of wavelengths contained in port N. Note that the same code type only occurs in 4 or more interference customers of dense distribution state. Appropriate ports should be allocated to these interference customers of dense distribution state to prevent the same code type. Besides, ports that contain less wavelengths should be allocated first to achieve a low degree of signal overlapping.

In 6-wavelength PON-LHDS, code allocation for 9 interference customers of dense distribution is listed in Table 1. At first, ports containing two wavelengths are chosen and allocated to interference customers, and then ports with more wavelengths are added in. There is no same code type existing in these 9 codes, thus any fault among these 9 customers, whether caused by one customer or several customers, will have its unique signal characteristic. However, in 6-wavelength PON-LHDS, if the number of interference customers is more than 9, the same code type will be inevitable.

TABLE 1. Code allocation for 9 interference Customers of Dense Distribution State.

Number of wavelengths	Port and code
2	2 (λ_5,λ_6), 3 (λ_4,λ_6), 5 (λ_3,λ_6), 9 (λ_2,λ_6), 17 (λ_1,λ_6)
3	7 (λ_3,λ_4,λ_6), 25 (λ_1,λ_2,λ_6)
4	26 (λ_1,λ_2,λ_5,λ_6)
6	32 (λ_1,λ_2,λ_3,λ_4,λ_5,λ_6)

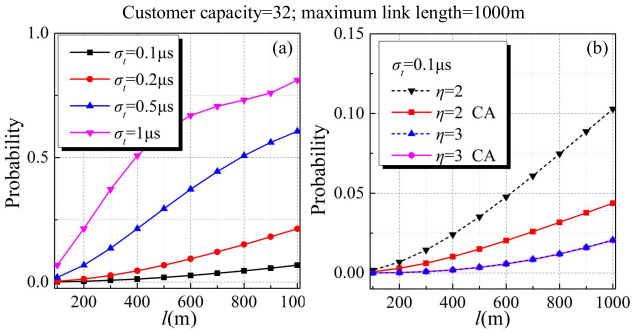

FIGURE 4. Customer interference probability of different σ_t versus link length: (a) σ_t from 0.1μs to 1μs; (b) code allocation (CA) effect.

IV. SIMULATION AND ANALYSIS

The probability of customer interference is affected by several network parameters such as the area of region, customer capacity, and the width σ_t of the failure-detecting light pulse. In Fig. 4 we study the impact of different values of σ_t on the probability of customer interference, while the maximum link length is 1000m, and customer capacity is 32. Under these circumstances, $E(2) = 284$, $E(3) = 60$, $E(4) = 5$, $E(5) = 1$, $E(6)$ and subsequent items are all zero. Fig. 4(a) shows that when σ_t is above 0.5μs, customer interference probability is much more than that of 0.2μs and 0.1μs, and customer interference is very severe. Obviously, reducing σ_t is one of the effective methods to achieve low probability of customer interference. Fig. 4(b) illustrates the probability of customer interference of different η (from 2 to 3) when σ_t equals to 0.1μs. When η equals to 2, 284 of all 496 pairs of codes have their characteristic wavelength, thus the customer interference probability is significantly reduced by the code allocation rule. When η is equal to or more than 3, since the cardinality of codes combinations is much larger than $E(\eta)$, the probability of customer interference is almost the same with that after code allocation. Fig. 5 illustrates the impact of customer capacity on the probability of customer interference. When network coverage is 2km^2 and σ_t is 0.1μs, in 32 and 128 customer system the probability of customer

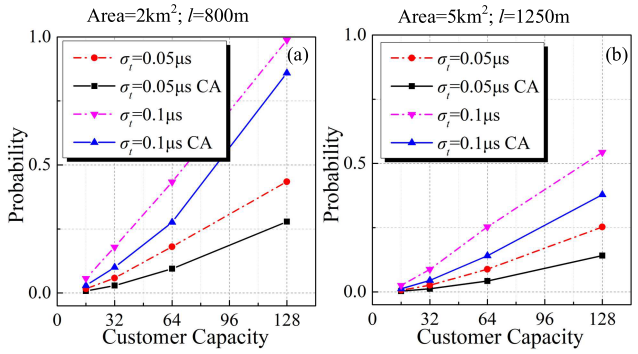

FIGURE 5. Customer interference probability of different σ_t versus customer capacity: (a) 2km^2 coverage with the link length of 800m; (b) 5km^2 coverage with the link length of 1250m.

interference is reduced by 0.079 and 0.129 after code allocation, respectively.

From the simulation results, we find that the code allocation rule achieves significant reduction of customer interference probability at different customer capacity. In the situation of high customer density, interference from more than three customers increases rapidly. However, the main purpose of code allocation for more than three customers is to reduce the signal overlapping degree and to prevent the same code type.

V. EXPERIMENTAL DEMONSTRATION

A. EXPERIMENTAL DEMONSTRATION OF CODE ALLOCATION

Experimental system has been set up to validate the proposed scheme. In the transmitter module, six directly modulated narrowband lasers of (λ_1, λ_2, λ_3, λ_4, λ_5, λ_6) within C band were used to generate the failure-detecting light pulses. The failure-detecting light pulses were sent into the 15km feeder fiber and then passed through a 32 customer 2D optical encoder to each customer. In the receiver module, six high sensibility optical receivers were used to detect the reflection signals. The link lengths of these 8 customers are 0.25km, 0.5km, 0.6km, 0.8km, 1km and 1.5km, and three of them are 1km. Therefore, two customers (C_1, 0.5km) and (C_2, 0.6km) of sparse distribution and three customers (C_3, C_4, C_5, 1km) of dense distribution are involved in the experimental system.

Fig. 6 shows the experiment results of 8 customers at different condition of σ_t. In Fig. 6(a), the codes of C_1 and C_2 are (λ_1, λ_2, λ_5, λ_6) and (λ_1, λ_2, λ_6). The codes of C_3, C_4 and C_5 are (λ_1, λ_3, λ_6), (λ_1, λ_5, λ_6) and (λ_3, λ_5, λ_6). Obviously, when σ_t equals to 1μs, except for λ_5 of C_1, the other signals of these 5 customers are overlapped. In Fig. 6(b), when σ_t reduces to 0.5μs, signals of C_1 and C_2 no longer overlap, but it doesn't change the situation of C_3, C_4 and C_5. In Fig. 6(c), their code distribution in the wavelength domain has changed after code allocation. Although signals of C_3 and C_5 overlap in channel λ_3, each customer is allocated a characteristic wavelength as its identity. By reducing the width of the failure-detecting light pulse and code allocation, the interference between these 8 customers is mitigated.

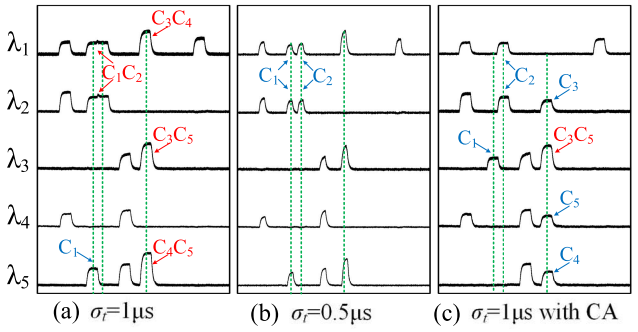

FIGURE 6. Signal sequence of 8 customers: (a) $\sigma_t = 1\mu$s; (b) $\sigma_t = 0.5\mu$s; (c) $\sigma_t = 1\mu$s with code allocation.

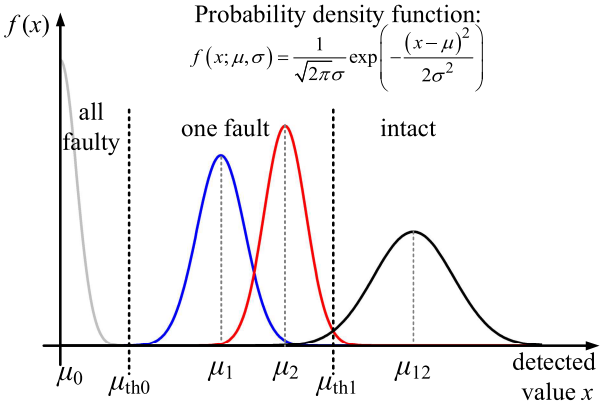

FIGURE 7. Thresholds for the link state signals of two interference customers.

B. LINK STATE DECISION CRITERION

To process the complex signals and obtain the accurate failure decision criterion for interference customers, four kinds of noise sources cannot be ignored in the system, including shot noise, dark current noise, thermal noise, and beat noise [20, 26]. Considering the partially or completely overlapping of interference customers, the detected value x, i.e., the integral of the link state signals $f(t)$ over the corresponding time-window $(0, \tau)$ is used to represent the link state:

$$x = \int_0^{\tau} f(t)dt \tag{7}$$

The detected value x and noise-related term σ are assumed to be Gaussian, and μ is the expected value of the link state. Fig. 7 illustrates the multi-stage thresholds for the link state signals of two interference customers. μ_0 stands for the state that two fiber links are faulty. μ_1 and μ_2 are the state that only one fiber link is faulty, and $\mu_1 < \mu_2$. μ_{12} represents that two fiber links are intact. μ_{th0} and μ_{th1} are the thresholds for three link states: all faulty, one fault and intact, as shown in Fig. 7. Here, we take the derivation of μ_{th1} as an example. We define σ_1, σ_2 and σ_{12} as the noise standard deviation of μ_1, μ_2 and μ_{12}, respectively. When $\mu_1 < \mu_2$, i.e. μ_{th1} is between μ_2 and μ_{12}, the impact of $f(x; \mu_2, \sigma_2)$ on the probability of detection is much larger than $f(x; \mu_1, \sigma_1)$, thus only

$f(x;\mu_2,\sigma_2)$ and $f(x;\mu_{12},\sigma_{12})$ are involved in the decision of μ_{th1}. The detection of one fault state is under the condition of $x < \mu_{\text{th1}}$. The detection probability P_D is the probability of correctly identifying the fault, and the false alarm probability P_F is that the intact state is misjudged into one fault state. Therefore, the detection probability P_D and the false alarm probability P_F can be derived by

$$P_D = \frac{1}{\sqrt{2\pi}\sigma_2} \cdot \int_{-\infty}^{\mu_{th1}} e^{-\frac{(x-\mu_2)^2}{2\sigma_2^2}} dx$$
$$P_F = \frac{1}{\sqrt{2\pi}\sigma_{12}} \cdot \int_{-\infty}^{\mu_{th1}} e^{-\frac{(x-\mu_{12})^2}{2\sigma_{12}^2}} dx \quad (8)$$

The threshold is to make P_D as high as possible and P_F as low as possible. Therefore, the optimal threshold is obtained, when $P_D - P_F$ reaches its maximum value. The optimal threshold can be written as

$$\mu_{th1} = \frac{b - \sqrt{b^2 - 4ac}}{2a}$$
$$a = \sigma_{12}^2 - \sigma_2^2, \quad b = 2\mu_2\sigma_{12}^2 - 2\mu_{12}\sigma_2^2,$$
$$c = \mu_2^2\sigma_{12}^2 - \mu_{12}^2\sigma_2^2 - 2\sigma_2^2\sigma_{12}^2 \ln\frac{\sigma_{12}}{\sigma_2} \quad (9)$$

However, the received link state signals $f(t)$ depend on the location of the encoders, the loss for each channel, the peak power of the failure-detecting light pulse, the loss difference between the ports of the FBG encoder, and the dynamic interaction process between the failure-detecting light pulse and FBG encoder due to the central wavelength shift, etc. With the known conditions of system parameters including the light sources, FBG encoder, link lengths and other passive optical components, the expected value μ can be derived by the equation of dynamic interaction process in [21]. All the factors mentioned above lead to the difference of the link state signals between different customers, which will bring difficulties in the thresholds partition. In the actual deployment of 2D optical coding PON LHDS, the code allocation contributes to reduce the overlapping degree of interference customers, so as to easily obtain the accurate decision criterion for link state recognition.

VI. CONCLUSION

To process the complex link state signals and obtain the accurate failure decision criterion for massive densely distributed customers, customer interference issues in the deployment of 2D optical coding PON-LHDS are investigated in this paper. A customer probability distribution model based on uniform distribution is proposed, and the impact of system parameters: the width of the failure-detecting light pulse, customer capacity and the area of network coverage on the customer interference probability is derived. Interference customers are divided into two distribution states: dense and sparse distribution states, based on the signal overlapping of interference customers. For different distribution states of interference customers, the code allocation rule is proposed to reduce the customer interference probability and prevent potential false alarm by changing the connection between the output ports of encoder and access customers. The simulation results show that in 128 customer system with 2km^2 coverage and 0.1μs width of the failure detecting light pulse, customer interference probability is reduced by 0.129 after code allocation. The feasibility of the code allocation rule is demonstrated by experiment that the interference between 5 customers of two distribution states is eliminated after code allocation. Besides, the link state partition for interference customers is derived to process the overlapping interference signals. In conclusion, the code allocation rule and precise link states partition combined with proper width of the failure-detecting light pulse help to improve the accuracy of 2D optical coding PON-LHDS.

REFERENCES

[1] D. Nesset, "NG-PON2 technology and standards," *J. Lightw. Technol.*, vol. 33, no. 5, pp. 1136–1143, Mar. 1, 2015.

[2] H. S. Abbas and M. A. Gregory, "The next generation of passive optical networks: A review," *J. Netw. Comput. Appl.*, vol. 67, pp. 53–74, May 2016.

[3] M. M. Rad, K. Fouli, H. A. Fathallah, L. A. Rusch, and M. Maier, "Passive optical network monitoring: Challenges and requirements," *IEEE Commun. Mag.*, vol. 49, no. 2, pp. S45–S52, Feb. 2011.

[4] P. J. Urban, G. C. Amaral, G. Żegliński, E. Weinert-Raczka, and J. P. von der Weid, "A tutorial on fiber monitoring for applications in analogue mobile fronthaul," *IEEE Commun. Surveys Tutr.*, vol. 20, no. 4, pp. 2742–2757, 4th Quart., 2018.

[5] M. P. Fernández, L. A. B. Rossini, J. P. Pascual, and P. A. C. Caso, "Enhanced fault characterization by using a conventional OTDR and DSP techniques," *Opt. Express*, vol. 26, no. 21, p. 27127, Oct. 2018.

[6] G. C. Amaral, L. E. Y. Herrera, D. Vitoreti, G. P. Temporão, P. J. Urban, and J. P. von der Weid, "WDM-PON monitoring with tunable photon counting OTDR," *IEEE Photon. Technol. Lett.*, vol. 26, no. 13, pp. 1279–1282, Jul. 1, 2014.

[7] P. J. Urban, G. Vall-llosera, E. Medeiros, and S. Dahlfort, "Fiber plant manager: An OTDR- and OTM-based PON monitoring system," *IEEE Commun. Mag.*, vol. 51, no. 2, pp. S9–S15, Feb. 2013.

[8] A. T. Liem, I.-S. Hwang, A. Nikoukar, and M. S. Ab-Rahman, "Distribution drop fiber in-service fault management in enhanced EPON system," *Opt. Switching Netw.*, vol. 17, pp. 52–63, Jul. 2015.

[9] M. A. Esmail and H. Fathallah, "Physical layer monitoring techniques for TDM-passive optical networks: A survey," *IEEE Commun. Surveys Tutr.*, vol. 15, no. 2, pp. 943–958, 2nd Quart., 2013.

[10] S. Hann, J.-S. Yoo, and C.-S. Park, "Monitoring technique for a hybrid PS/WDM-PON by using a tunable OTDR and FBGs," *Meas. Sci. Technol.*, vol. 17, no. 5, pp. 1070–1074, May 2006.

[11] L. Baudzus and P. Krummrich, "CDM-Based λ-OTDR for rapid TDM- and WDM-PON monitoring," *IEEE Photon. Technol. Lett.*, vol. 26, no. 12, pp. 1203–1206, Jun. 15, 2014.

[12] Y. Yuan, W. Li, J. Han, Q. Feng, H. Yao, Q. Zheng, Q. Hu, and S. Yu, "Fault monitoring in passive optical network using code division multiplex-based dual-OTDR traces comparison," *Chin. Opt. Lett.*, vol. 15, no. 3, pp. 83–87, Jan. 2017.

[13] H. Fathallah, M. M. Rad, and L. A. Rusch, "PON monitoring: Periodic encoders with low capital and operational cost," *IEEE Photon. Technol. Lett.*, vol. 20, no. 24, pp. 2039–2041, Dec. 15, 2008.

[14] M. M. Rad, H. A. Fathallah, S. LaRochelle, and L. A. Rusch, "Computationally efficient monitoring of PON fiber link quality using periodic coding," *J. Opt. Commun. Netw.*, vol. 3, no. 1, pp. 77–86, Jan. 2011.

[15] M. P. Fernandez, P. A. Costanzo Caso, and L. A. Bulus Rossini, "False detections in an optical coding-based PON monitoring scheme," *IEEE Photon. Technol. Lett.*, vol. 29, no. 10, pp. 802–805, May 15, 2017.

[16] X. Zhou, F. Zhang, and X. Sun, "Centralized PON monitoring scheme based on optical coding," *IEEE Photon. Technol. Lett.*, vol. 25, no. 9, pp. 795–797, May 1, 2013.

[17] A. O. P. Sousa, C. A. F. Marques, R. Nogueira, and P. S. André, "Simplified method for passive optical network in-service fibre-fault monitoring based on fibre Bragg gratings," *Photon. Netw. Commun.*, vol. 34, no. 1, pp. 149–154, Aug. 2017.
[18] M. P. Fernandez, L. A. Bulus Rossini, and P. A. Costanzo Caso, "PON monitoring technique using single-FBG encoders and wavelength-to-time mapping," *IEEE Photon. Technol. Lett.*, vol. 31, no. 21, pp. 1745–1748, Nov. 1, 2019.
[19] X. Zhang and X. Sun, "Optical pulse width modulation based TDM-PON monitoring with asymmetric loop in ONUs," *Sci. Rep.*, vol. 8, no. 1, p. 4472, Dec. 2018.
[20] X. Zhang, F. Lu, S. Chen, X. Zhao, M. Zhu, and X. Sun, "Remote coding scheme based on waveguide Bragg grating in PLC splitter chip for PON monitoring," *Opt. Express*, vol. 24, no. 5, p. 4351, Mar. 2016.
[21] Z. Ge, S. Chen, and X. Sun, "Dynamic interaction process analysis between failure-detecting light pulse and 2D optical encoder in link health detection system for PON," *J. Lightw. Technol.*, vol. 37, no. 3, pp. 1063–1069, Feb. 1, 2019.
[22] M. D. Vaughn, D. Kozischek, D. Meis, A. Boskovic, and R. E. Wagner, "Value of reach-and-split ratio increase in FTTH access networks," *J. Lightw. Technol.*, vol. 22, no. 11, pp. 2617–2622, Nov. 2004.
[23] M. Rad, H. Fathallah, and L. Rusch, "Fiber fault PON monitoring using optical coding: Effects of customer geographic distribution," *IEEE Trans. Commun.*, vol. 58, no. 4, pp. 1172–1181, Apr. 2010.
[24] K. V. Rohatgi and A. K. Md Ehsanes Saleh, "Uniform distribution," in *An Introduction to Probability and Statistics*, 3rd ed. Hoboken, NJ, USA: Wiley, 2015, pp. 199–201.
[25] X. Zhang, S. Chen, F. Lu, X. Zhao, M. Zhu, and X. Sun, "Remote coding scheme using cascaded encoder for PON monitoring," *IEEE Photon. Technol. Lett.*, vol. 28, no. 20, pp. 2183–2186, Oct. 15, 2016.
[26] M. Rad, H. Fathallah, and L. Rusch, "Performance analysis of fiber fault PON monitoring using optical coding: SNR, SNIR, and false-alarm probability," *IEEE Trans. Commun.*, vol. 58, no. 4, pp. 1182–1192, Apr. 2010.

ZHIQUN GE was born in Jiangsu, China, in 1989. He received the B.S. and M.A. degrees in electronics engineering from Southeast University, Nanjing, China, in 2011 and 2015, respectively, where he is currently pursuing the Ph.D. degree in electronics engineering with the National Research Center for Optical Sensing/Communications Integrated Networking. His research interests include optical fiber communications and optical network monitoring.

XIAOHAN SUN is currently working as a Professor with the School of Electronic Science and Engineering and the Director of the National Research Center for Optical Sensing/Communications Integrated Networking, Southeast University, Nanjing, China. She was a Visiting Professor with the Research Laboratory of Electronics, Massachusetts Institute of Technology, Cambridge, MA, USA, from 2002 to 2004. Her current research interests include photonic/electronic integrated chips and devices, optical sensing, and next-generation optical networks.